Materials Physics and Mechanics 27 (2016) 74-78 Received: April 7, 2016

SIMULATION OPERATION REGIMES OF PASSIVE MODE-LOCKED LASER BASED ON InGaAlAs/InGaAs/InP HETEROSTRUCTURES

I.S. Polukhin[1*], G.A. Mikhailovskiy[1], D.A. Rybalko[1], Yu.V. Solov'ev[1], M.A. Odnoblyudov[1], A.E. Gubenko[1], D.A. Livshits[1], A.N. Firsov[1], A.N. Kirsyaev[1], A.A. Efremov[1], V.E. Bougrov[2]

[1]Peter the Great St. Petersburg Polytechnic University, Saint Petersburg, 195251, Russia

[2]ITMO University, Saint Petersburg, 197101, Russia

*e-mail: ivanpolukhin@yandex.ru

Abstract. We propose a model of passive mode-locking laser diode based on quantum wells. Numerical results for InGaAlAs/InGaAs/InP heterostructure with 4 quantum wells in active region are presented. The dynamics of the transition to mode-locking has been investigated. It has been shown that mode-locking occurs approximately within 30 ns. The pulse duration was amounted to 2 ps, average output power - to 9.4 mW. The appearance of the second harmonic radiation in the resonator is connected to the insufficient absorber relaxation rate.

1. Introduction

Passive mode-locked lasers are high-potential sources for the generation of ultrashort pulses used both in fundamental research and application. In addition, the passive mode-locked lasers are part of the element base for radio photonics [1, 2] and, particularly, can be used for adjusting the sampling frequency in radio-photonic analog-to-digital converters [3]. Passive mode-locking can be deployed in any kind of lasers, such as gas, liquid organic dyes or semiconductor heterostructure ones. However, the semiconductor lasers have advantages in comparison with the others due to small size, low energy consumption and low threshold currents. Also, the semiconductor lasers can be easily integrated into electronics. In terms of design the passive mode-locked heterolaser consists of the following two sections: a gain section which is biased in straight direction and a reverse-biased saturable absorber made of the same material as the gain medium. Today the passive mode-locked lasers are successfully deployed in quantum dots and wells for 1.3-1.55 μm wave length range on GaAs and InP substrates [4-6]. This spectral range is used for optical communication lines due to minimum losses in quartz optical fibre and the possibility to work in wavelength-division multiplexing. Also, EDFA amplifiers for this particular bandwidth are already being produced. Multiple-layer semiconductor heterostructures based on InP substrates are used in order to generate radiation at 1.55 μm wavelength. Nevertheless, this causes a number of difficulties connected to technologic growth of structures consisting of phosphorus. Thus, phosphorus-free structures are of the most interest [5]. Here we simulate a heterostructure that contains phosphorus only in substrate for the purpose of generation of laser radiation in the passive mode-locking. The aim of this work is to create a simulation model of passive mode-locked laser based on quantum wells and calculate InGaAlAs/InGaAs/InP heterostructures using the model under consideration for further practical application.

2. Model

This model allows to define the main laser specifications, such as pulse repetition rate, pulse shape/width and power. Passive mode-locking models can be divided into two groups as follows: electromagnetic field equation depending on time and electromagnetic field equation depending on frequency [7-9]. Models with frequency-based equations can be advantageous in terms of time for numerical calculations [7]. Here we use a model which describes how electromagnetic field is changed in time since it is less complicated for understanding the mode-locking processes. Such models are based on travelling wave equations which shall be completed with boundary conditions, which link amplitudes at the boundaries of different laser sections and initial conditions responsible for the first pulse of laser radiation. Here we accompany the wave equation with a spontaneous noise function that is responsible for the initial generation of laser radiation. The spontaneous noise function is complex, random both in space and time while having no correlation between the real and imaginary parts. The distribution density of such parts is described by a Gaussian distribution.

The wave linearly-polarized complex field can be distributed into components that propagate in the opposite directions,

$$E(r,t) = \Phi(x,y)\exp(-i\omega_0 t)(E^+(z,t)\exp(ik_0 z) + E^-(z,t)\exp(-ik_0 z)),$$

where $E^+(z,t)$ and $E^-(z,t)$ are the amplitudes of the counter-propagating waves, $\Phi(x,y)$ – lateral mode section, ω_0 – carrier wave frequency, k_0 – wave vector. Having defined a certain wavelength λ_0, the field inside the resonator ($0 \le z \le L$, where L – resonator length) presents slowly varying amplitudes in space $\left|\frac{1}{E^\pm}\frac{\partial E^\pm}{\partial z}\right| \ll k_0$ and time – $\left|\frac{1}{E^\pm}\frac{\partial E^\pm}{\partial t}\right| \ll \omega_0$, then the travelling wave equations in a laser with absorption and gain sections can be written as follows [10, 11]:

$$\frac{\partial E^+}{\partial t} + v_g\frac{\partial E^+}{\partial z} = v_g\frac{\Gamma\sigma(n-n_t)}{2}(1-i\alpha_H)E^+ + \Gamma\frac{v_g\sigma n_t}{2\omega_g^{\,2}}\frac{\partial^2 E^+}{\partial t^2} - v_g\frac{\alpha_i}{2}E^+ + F_{sp}^+, \quad (1)$$

$$\frac{\partial E^-}{\partial t} - v_g\frac{\partial E^-}{\partial z} = v_g\frac{\Gamma\sigma(n-n_t)}{2}(1-i\alpha_H)E^- + \Gamma\frac{v_g\sigma n_t}{2\omega_g^{\,2}}\frac{\partial^2 E^-}{\partial t^2} - v_g\frac{\alpha_i}{2}E^- + F_{sp}^-, \quad (2)$$

where v_g – group velocity, α_i – internal loss index, Γ – optical confinement factor, i. e. electromagnetic radiation fraction which is distributed along the active region of laser structure, σ – differential gain or absorption (depending on a section), n_t – concentration at transparency threshold, α_H – Henry-factor at transparency threshold [12], ω_g – frequency gain dispersion rate, F_{sp} – spontaneous noise function responsible for the initial generation of radiation since there are no photons in the resonator at the initial moment.

A member with the second time derivative of change $E^\pm$ considers frequency gain dispersion and is derived from parabolic expansion of gain rate depending on the frequency near the maximum. Counter-propagating wave amplitudes at the resonator boundaries are linked through amplitude mirror ratios.

$$\begin{aligned} E^+(0,t) &= r_0 E^-(0,t), \\ E^-(L,t) &= r_L E^+(L,t), \end{aligned} \quad (3)$$

where r_0 and r_L – amplitude reflection coefficient of mirror ratios from the direction of absorption section (r_0) and from the direction of gain section (r_L). The chosen field amplitude unit must ensure the compliance of sum $\left|E^+\right|^2 + \left|E^-\right|^2$ and local photon concentration. This model

implies that gain maximum equals carrier frequency ω_0, group velocity dispersion is considered negligibly low. Equations (1)-(3) shall be complemented with a rate equation which considers carrier injection into ground state of a quantum well, recombination losses and interaction with the optical field through stimulated transitions.

$$\frac{\partial n}{\partial t} = \frac{I(z)}{eV} - \begin{cases} Dn + v_g \sigma_a (n - n_t)(\left|E^+\right|^2 + \left|E^-\right|^2) \\ An + Bn^2 + Cn^3 + v_g \sigma_g (n - n_t)(\left|E^+\right|^2 + \left|E^-\right|^2) \end{cases}, \quad (4)$$

the first brace-enclosed equation here refers to absorption section, the second one – to gain section, e – the elementary charge, V – volume of active region, σ_a, σ_g – differential absorptions, gain A – nonradiative recombination coefficient, B – radiative recombination coefficient, C – Auger recombination coefficient, D – absorber saturation rate, $I(z)$ – pumping current which is 0 for absorption section and I_G for gain section.

Equations (1)-(4) make a closed equation system that enables to determine repetition rate, as well as width and shape of the pulse. The output power can be calculated using the following formula:

$$Power[W] = \hbar w_0 \left|E^+\right|^2 v_g \frac{V}{L \cdot \Gamma}(1 - R_L), \quad (5)$$

where $\hbar$ – the Planck constant, R_L – reflection factor of one of the mirrors.

3. Simulated heterostructure

This model describes a heterostructure-based strip-geometry laser consisting of 4 InGaAlAs/InGaAs quantum wells grown on InP substrate. Structure topological parameters were calculated earlier [13] and were used here. The simulated structure parameters are given in the table below.

Table. Simulated structure parameters.

No.	Parameter name	Symbol	Value	Unit of measure-ment
1	Group velocity	v_g	$0.91\ 10^{10}$	cm/s
2	Resonator overall length	L	0.455	cm
3	Absorber length	l_a	0.0455	cm
4	Internal loss rate	α_i	5	cm^{-1}
5	Optical confinement factor	Γ	0.025	
6	Differential gain	σ_g	$4\ 10^{-16}$	cm^2
7	Differential absorption	σ_a	$2\ 10^{-15}$	cm^2
8	Henry-factor [12]	α_H	2	
9	Transparency threshold concentration	n_t	10^{18}	cm^{-3}
10	Frequency gain dispersion rate	ω_g	$7.5\ 10^{13}$	s^{-1}
11	Nonradiative recombination coefficient [14]	A	$2\ 10^8$	s^{-1}
12	Radiative recombination coefficient [14]	B	$0.96 \cdot 10^{-10}$	cm^3/s
13	Auger recombination coefficient [14]	C	$7\ 10^{-29}$	cm^6/s
14	Absorber relaxation rate	D	10^{11}	s^{-1}
15	Absorption section bias voltage	U	0-4	V
16	Active region volume	V	$1.7\ 10^{-10}$	cm^{-3}

17	Waveguide spontaneous emission contribution [15]	β_{sp}	10^{-4}	
18	Amplitude reflection coefficient at 0 boundary	r_0	1	
19	Amplitude reflection coefficient at L-boundary	r_L	0.9	
20	Pumping current	I_G	300-900	mA

4. Results and Discussion

Analysis of simulation results has shown that passive mode-locking occurs when pumping currents exceed the threshold one by 2.5-3 times. Thus, two different pulse generation modes are possible depending on the negative bias applied to the absorber: second harmonic locking at a voltage of less than 2V (Fig. 1) and fundamental mode-locking at a voltage of more than 4V (Fig. 2). This is due to the increase of absorber relaxation rate since a greater negative voltage at the absorber leads to greater relaxation rate. A similar behaviour was observed in quantum dots structures and described in work [16].

The simulation model, as shown above, allows to track the dynamics of formation of ultrashort laser pulses in passive mode-locking. At the initial moment carrier concentration in the gain section reaches a transparency level while there are no carriers in the absorption section and a lightwave represents noise which is distributed along the resonator (Figs. 1, 2a).

Thus, over 5 ns many weak light pulses are formed (Figs. 1, 2b), which are individually not capable of saturating the absorber, but it is due to their quantity that the concentration of carriers grows in the absorber as well as the radiation intensity, without qualitative changes.

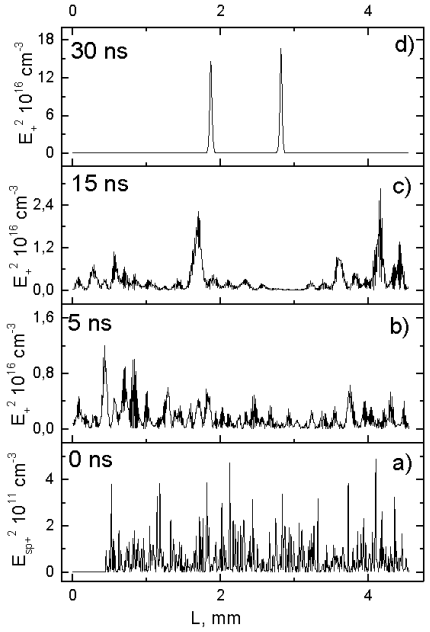

Fig. 1. Distribution of radiation intensity along the laser resonator in second harmonic mode-locking.

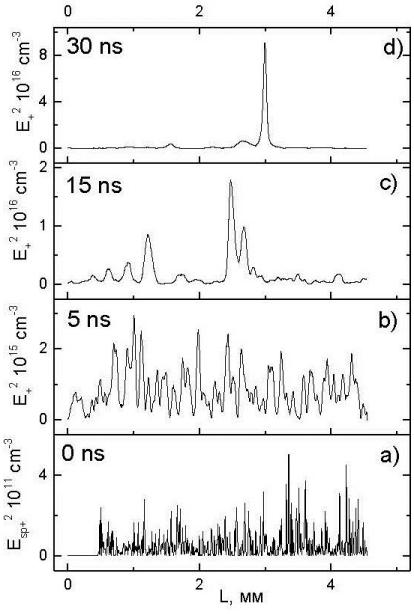

Fig. 2. Distribution of radiation intensity along the laser resonator in fundamental mode-locking.

Over the next 10 ns (at the moment of time of 15 ns (Figs. 1, 2c)) the light pulse intensity significantly grows and reaches the level where the most powerful pulses become capable of saturating the absorber. Over the next 5 ns the intensity of the most powerful pulses does not change while the intensity of the weak ones reduces by a factor of 5 times. From this point on the dynamics of development of different modes is different.

Thus, in second harmonic mode-locking the weak pulses completely disappear at the moment of time of 30 ns while the intensity of the two most powerful ones significantly grows followed by stationary floatation of the process. In fundamental mode-locking the intensity of

the most powerful pulse increases by a factor of 3 times at the moment of time of 30 ns while the spurious pulses have not been completely absorbed yet.

Thus, the simulation showed that the generation of pulses in the given structure can occur in two modes – fundamental and second harmonic. In fundamental passive mode-locking a single pulse of 2 ps long and 10 hHz repetition frequency is formed while the output radiation power equals 9.4 mW. In second harmonic mode-locking the radiation of pulses occurs at doubled frequency, impulse duration is 2 ps.

5. Conclusions

Here we have developed a simulation model of a passive mode-locked laser and tracked the dynamics of formation of pulse radiation. It has been shown that the two modes are possible in the given structure - fundamental and second harmonic.

In further research, we aim to include electron diffusion into the equation, consider intraband saturation process as well as conduct experimental research on laser structure with the above-mentioned parameters.

Acknowledgements. *This work supported by the Ministry of Education and Science of the Russian Federation as a part of federal purpose-oriented program "Researches and development works on priority direction of Russian scientific and technological complex for 2014-2020 years", code number 2015-14-579-0015, agreement No 14.578.21.0100, unique identifier RFMEFI57814X0100.*

References

[1] G.C. Valley // *Optics Express* **15** (2007) 1955.
[2] A. Khilo, S.J. Spector, E. Matthew, A.H. Nejadmalayeri, C.W. Holzwarth, M.Y. Sander, M.S. Dahlem, M.Y. Peng, M.W. Geis, N.A. DiLello, J.U. Yoon, A. Motamedi, J.S. Orcutt, J.P. Wang, C.M. Sorace-Agaskar, M.A. Popović, J. Sun, G.-R. Zhou, H. Byun, J. Chen, J.L. Hoyt, H.I. Smith, R.J. Ram, M. Perrott, T.M. Lyszczarz, E.P. Ippen, F.X. Kärtner, // *Optics Express* **20** (2012) 4454.
[3] R.S. Staricov // *Uspekhi Sovremennoi Radioelektroniki* **2** (2015) 3. (In Russian)
[4] T. Sadeev, D. Arsenijević, D. Franke, J. Kreissl, H. Künzel, D. Bimberg // *Applied Physics Letters* **106** (2015) 031114.
[5] Lianping Hou, Mohsin Haji, Bocang Qiu, Jehan Akbar, A. Catrina Bryce, John H. Marsh // *IEEE Photonics Technology Letters* **23** (2011) 1064.
[6] F. Gao, S. Luo, H.-M. Ji, S.-T. Liu, D. Lu, Ch. Ji, T. Yang // *Optics Communications* **370** (2016) 18.
[7] E.A Avrutin, J.H. Marsh, E.L. Portnoi // *Proceedings-Optoelectronics* **147** (2000) 251.
[8] M. Radziunas, A. G. Vladimirov, E.A. Viktorov, G. Fiol, H. Schmeckebier, D. Bimberg // *IEEE Journal of Quantum Electronics* **47(7)** (2011) 935.
[9] A.G. Vladimirov, D. Turaev // *Physical Review A* **72** (2005) 033808.
[10] G.P. Agrawal, *Nonlinear Fiber Optics* (Academic Press, San-Diego, 2001).
[11] P. Vankwikelberge, G. Morthier, R. Baets // *IEEE Journal of Quantum Electronics* **26** (1990) 1728.
[12] C.H. Henry // *IEEE Journal of Quantum Electronics* 18 (1982) 259.
[13] G.A. Mikhailovskiy, I.S. Polukhin, D.A. Rybalko, Yu.V. Solov'ev, M.A. Odnoblyudov // *Technical Physics Letters* **42(9)** (2016) 56. (In Russian).
[14] Yu.A. Goldberg, N.M. Schmidt, In: *Handbook Series on Semiconductor Parameters*, Vol. 2, ed. by M. Levinshtein, S. Rumyantsev, M. Shur (World Scientific, London, 1999).
[15] A. Fali, E. Rajaei, Z. Kaftroudi // *Journal of the Korean Physical Society* **64** (2014) 16.
[16] M. Radziunas, A.G. Vladimirov, E.A. Viktorov // *Proceedings of SPIE* **7720** (2010) 77200X-1.